Surface & Coatings Technology 268 (2015) 216–223

Contents lists available at ScienceDirect

Surface & Coatings Technology

journal homepage: www.elsevier.com/locate/surfcoat

On the search for producing intermetallics by diffusion reaction of cold spray bulk deposits

Vít Jan *, Jan Čupera, Jan Cizek

Brno University of Technology, Faculty of Mechanical Engineering, Institute of Materials Science and Technology, The NETME Centre, Technická 2896/2, 61669 Brno, Czech Republic

ARTICLE INFO

Available online 10 December 2014

Keywords:
Cold spray
Reaction diffusion
Intermetallics
Reaction sequence
Bulk deposits

ABSTRACT

Bi-metallic mixtures of elemental powders were deposited by cold spray technique in the form of bulk, self-supportive deposits with thickness of about 8 mm. The combinations used were Ti–Al, Fe–Al and Ni–Al in 1:1 at.% composition. Aluminides of titanium, iron and nickel draw substantial attention as materials with high application potential but also substantial production technology complications. Therefore the bi-metallic deposits were subjected to extensive series of annealing experiments in order to assess their behaviour during reaction diffusion synthesis of intermetallic phases. Short annealing for 2 h was used in 4.8 Argon protective atmosphere. Metastable and according to PD stable phases were identified alongside with heterogeneous diffusion artefacts (e.g. porosity). Temperatures ranging from 350 °C to 600 °C were used, which provided both solid-state reactions and diffusion in locally melted aluminium part of the bi-metallic deposit.
The evolved phases were identified using X-Ray diffraction, local chemical microanalysis by EDS and the morphology was studied using light and electron microscopy. Although homogeneous material has not been achieved, the results are discussed with the aim for understanding and possible controlling of the reaction and homogeneity of the resulting material. Also materials in as deposited state were evaluated for deposition efficiency, and porosity.

1. Introduction

Intermetallics present an interesting group of materials with some outstanding qualities. In general, they possess high strength and low ductility — characteristics that are connected to their crystal lattice type. Aluminides are one important intermetallic group also from the mechanical point of view and are considered to have high potential as materials for high temperature application with good strength/density ratio [1,2].

These materials are usually manufactured using casting technologies such as precision casting under protective atmosphere or vacuum and limited machining. To test the possibility of overcoming this demanding process, the cold spray technique is used to form massive deposits with arbitrary shapes from heterogeneous bi-metallic mixtures [3–7].

Cold spray (CGDS) is a technique using pressurised gas as a carrier medium which expands in Laval-type nozzle to super-sonic speeds thus accelerating individual particles of the deposited powder. These weld locally upon impact on the substrate or previously deposited particles. The fact that the particles are not melted during flight and at impact and that oxidation of the particle surface is minimal establishes this method not only as surface engineering method but also as a bulk material deposition method, where high volumes of material can be deposited [8–11]. When comparing CGDS with classical powder metallurgy techniques that could be used for producing solids from powder mixtures, the main advantage lies in the possibility to produce arbitrary shapes with few limits in size and complexity of the shape. Using always the same depositing apparatus and preferably robotic arm, arbitrary powder mixtures can be used; even the possibility of changing the chemical composition of the feedstock during deposition can be considered.

2. Experimental setup

Cold spray technique was used to deposit the analysed material. Powder blends mixed in 50/50 at.% ratio from commercial pure Al, Ni, Fe and Ti powders were used as feedstock. Powders were purchased from GTV and HC Starck. Air was used as the carrier gas at a temperature of 300 °C and pressure of 15 bar. Samples in the form of bars were deposited by 20 or more consecutive passes of the nozzle. The resulting material had thickness of approximately 10 mm (Fig. 1).

The deposited materials were cut using a low speed saw to dimensions 5 × 6 × 7 mm and were then used for the annealing experiments

* Corresponding author.
E-mail address: jan@fme.vutbr.cz (V. Jan).

http://dx.doi.org/10.1016/j.surfcoat.2014.12.011
0257-8972/

a)

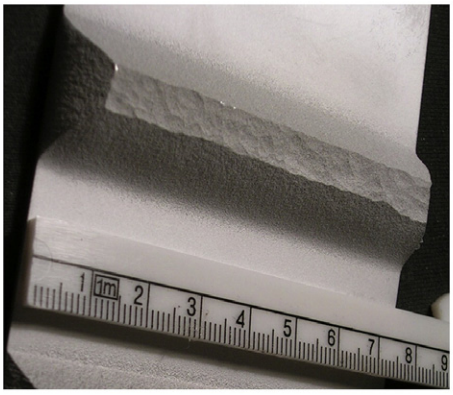

b)

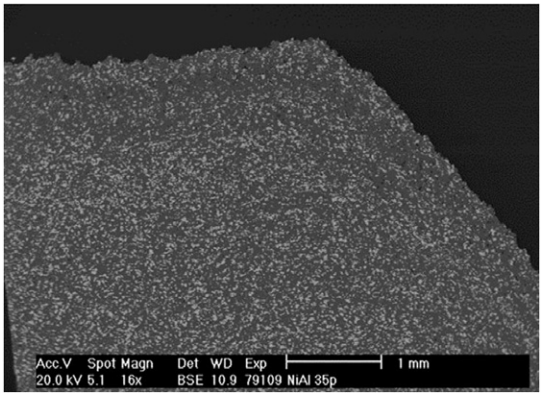

Fig. 1. a) Overall appearance of the deposited material and b) microstructure of the deposit.

under Ar protective atmosphere (flow of 0.5 l/min, 4.8 purity). The temperature was measured directly in the contact with samples using a thermocouple mounted in the sample holder. The substrate, which was commercially pure aluminium sheet, was removed before annealing, so that only the deposited bi-metallic CS deposit was annealed.

The following temperatures were used: 300 °C, 450 °C, 500 °C, 550 °C, and 600 °C. The temperatures were set according to DSC analysis results of the deposited materials to use the temperature range preceding the strong exothermic reaction occurring in the 625 °C to 650 °C range (Fig. 2). The experimental temperatures were kept below the main exothermic reaction temperature in order to secure maximum portion of the undergoing reactions to be a solid state diffusion reactions and not reactions between solid and melt in some mushy state. Due to the high amounts of heat evolved during the main exothermic reactions and the speed of these reactions it is not possible to control the amount of heat added in the sample and melting could occur at least locally.

All samples were rapidly heated to the selected temperatures by placing them into the hot zone of the pre-heated furnace; 2 h dwell times were used for the isothermal annealing. Following the annealing, the samples were moved out from the hot zone, but still left in the protective Ar atmosphere until they cooled to less than 100 °C. The samples were then left to cool freely in air.

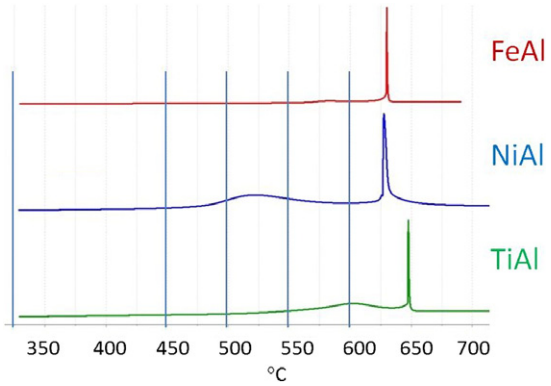

Fig. 2. DSC curves of the analysed materials, upwards is the direction of exothermic peaks.

The annealed samples were half-cut by a low speed saw and fractured. One part of each of the fractured specimens was used to prepare a metallographic sample by standard grinding and polishing techniques. No etching was used, but colloid silica (OPS from Struers) was used for the last polishing step to visualise the microstructure. The second half pieces of the respective samples were used for fracture surface characteristics. Light microscopy and electron microscopy were used to evaluate the fracture surfaces and the polished metallographic samples (Zeiss Z1M light microscope, Zeiss UltraPlus FEG-SEM). For the chemical analysis, local and mapping EDS analyses were used (OXFORD EDS). Setaram SetsysEvo DSC was used for the initial thermal analysis.

3. Analysis results

3.1. As-deposited materials

The microstructure of the as-deposited material consisted of aluminium matrix and nickel, titanium or iron individual grains which corresponded to the original individual powder particles. The deposited materials showed a shift in the chemical composition favouring aluminium in Ni–Al and Fe–Al systems and favouring titanium in Ti–Al system (Table 1). The as-deposited microstructure of the samples exhibited a porosity of 0.4% (Ti–Al), 0.3% (Ni–Al) and 0.3% (Fe–Al), respectively (Fig. 3).

On the fracture surfaces the severely deformed aluminium matrix exhibited ductile fracture, while the heavier particles delaminated from the Al matrix (Fig. 4).

Table 1
Overview of changes in chemical composition between feedstock and as-deposited material; measured by image analysis on light microscopy images taken by 100× total magnification.

	Composition of feedstock powder mixture (%)		Composition of as deposited material (%)		
	Atomic	Weight	Image analysis ratio	Weight	Atomic
Ti–Al					
Al	50	36	33.7	23	35
Ti	50	64	66.3	77	65
Ni–Al					
Al	50	31	79.9	55	72
Ni	50	69	20.1	45	28
Fe–Al					
Al	50	33	73.4	49	66
Fe	50	67	26.6	51	34

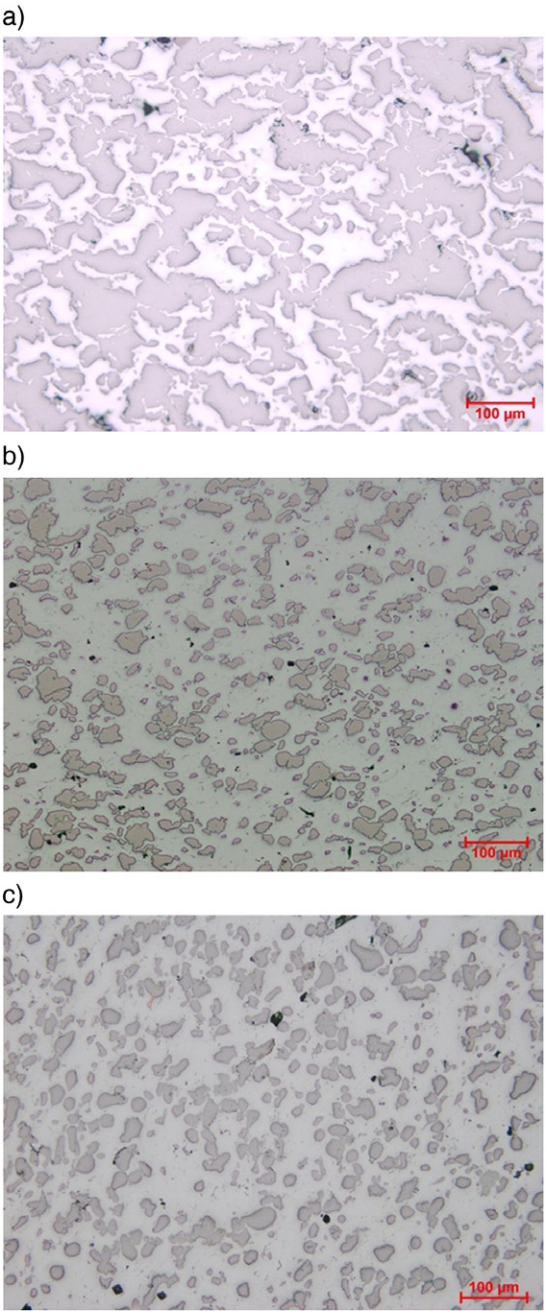

Fig. 3. Microstructure of the as deposited materials a) TiAl, b) NiAl and c) FeAl.

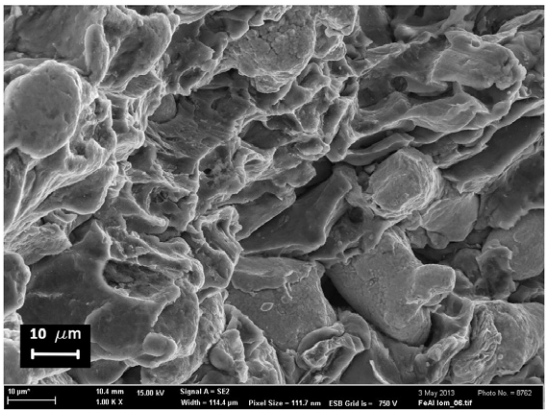

Fig. 4. A typical fracture surface of the as deposited material (FeAl). Delamination between Al particles showing ductile fracture and not fractured Fe particles.

3.2. Annealed Ti–Al deposits

The Ti–Al deposits exhibited first minor intermetallic phase occurrence after 300 °C of annealing (Fig. 5). Layer of TiAl mixtures formed at the Al–Ti particle interface when temperature was increased. Gradual formation of the $TiAl_3$ intermetallic phase started with 450 °C annealing. Samples annealed at 550 °C showed distinctive areas of the intermetallic phase formation at the original Ti–Al grain interface and also inside the titanium areas. These likely are connected to diffusion paths along boundaries between originally individual titanium particles. Some newly formed porosity can be seen at 550 °C and interconnected porosity has evolved after annealing at 600 °C/2 h when also local melting could be identified (Fig. 6). Even at 600 °C areas of pure unaffected titanium could be identified, while no pure aluminium areas were found in the microstructure (Figs. 7, 8).

3.3. Annealed Ni–Al deposits

The Ni–Al CGDS deposits exhibited first intermetallic formation of Ni_2Al_3 phase after 450 °C (Fig. 9). At 500 °C, concentric layers of Ni_2Al_3, NiAl and $NiAl_3$ intermetallic phases with gradually changing chemical proportions of nickel and aluminium formed on the nickel particles (Fig. 10). Sample annealed at 550 °C showed distinctive areas of the Ni_2Al_3 and $NiAl_3$ intermetallic phases with interconnected porosity (Fig. 11). The pores are comparable in size with the original powder particles. Un-reacted nickel particle cores were still visible after 550 °C. During annealing at 600 °C/2 h, a local melting most likely occurred based on the character of the microstructure (Fig. 12). The porosity has coarsened into smaller number of bigger pores (Fig. 13).

3.4. Annealed Fe–Al deposits

Newly formed Al_5Fe_2 phases were identified in the material only after annealing at temperatures starting at 500 °C (Fig. 14). Only minor part of the iron particles reacted after 2 h of annealing. Annealing at 600 °C created FeAl and $FeAl_2$ phases with a substantial porosity (Figs. 15, 16). The material changed its character into open interconnected porosity structure (Fig. 17). The outer shape of the sample was maintained, although the macroscopic dimensions of the sample increased. Some remnants of un-reacted iron could be seen in the microstructure.

4. Discussion

The as deposited materials after cold spraying showed change in chemical composition when compared to the ratio of the used stock mixture. Different deposition efficiencies of the metal pairs at the given deposition conditions are evident. The Ti–Al mixture favoured titanium whereas the other two mixtures — Ni–Al and

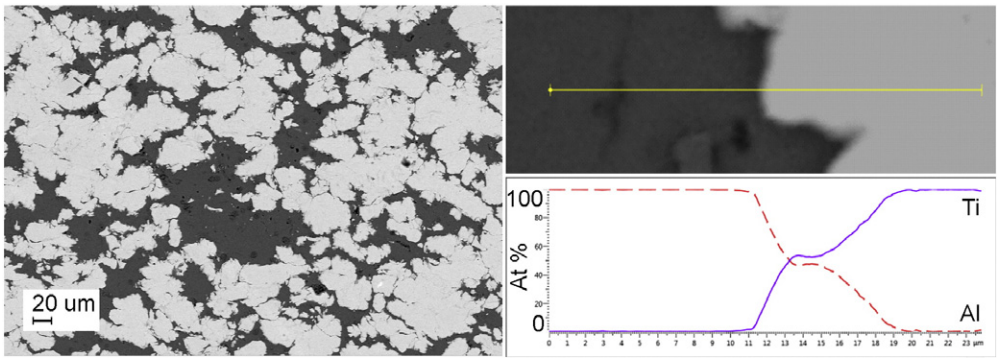

Fig. 5. Microstructure and detail of Ti–Al interphase with linear EDX analysis showing evolution of TiAl intermetallic phase after 2 h annealing at 300 °C.

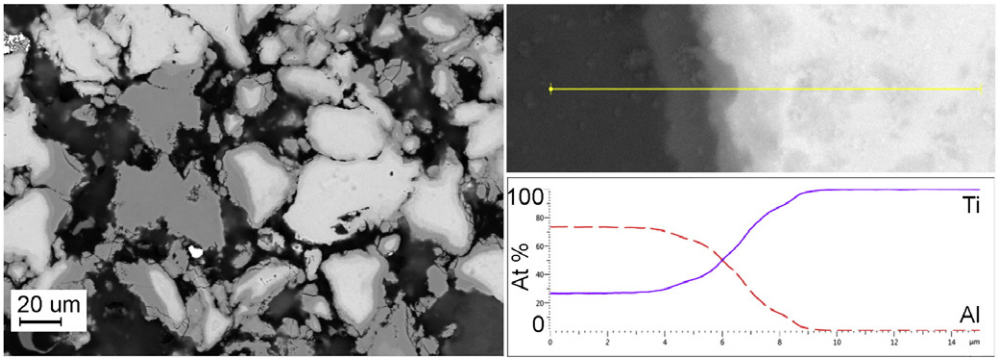

Fig. 6. Microstructure and detail of gradual interphase between titanium particle and $TiAl_3$ phase with linear EDX analysis showing evolution of intermetallic phase after 2 h annealing at 600 °C.

Fe–Al favoured aluminium (Fig. 18). The Ti–Al change is in agreement with the results reported in [7] where also enrichment in titanium is reported. Different behaviours showing enrichment in Ni for the Ni–Al system were reported in [12] for lower deposition pressures.

Intermetallic phases formed in all of the studied CGDS deposits once sufficient temperature was reached (Table 2). The gradual evolution of different phases generally can be connected with the known binary phase diagrams, however some of the phases, although very prominent in the chemical analysis, are not mentioned in the stable phase diagrams

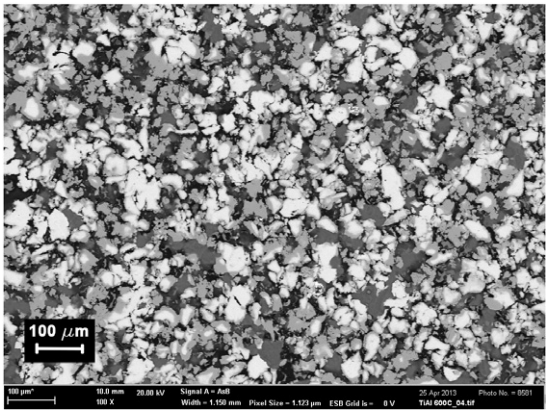

Fig. 7. Microstructure of the Ti–Al deposit after 600 °C/2 h.

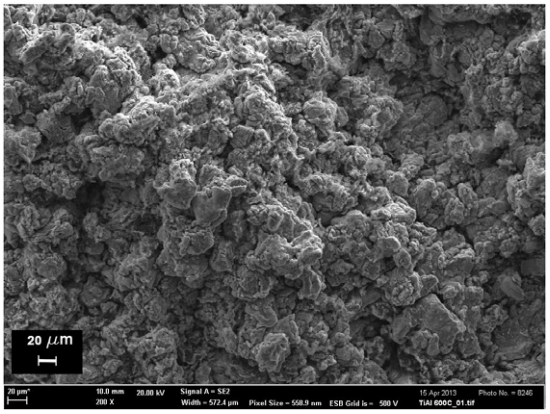

Fig. 8. Fracture surface with porosity of the Ti–Al deposit after 600 °C/2 h.

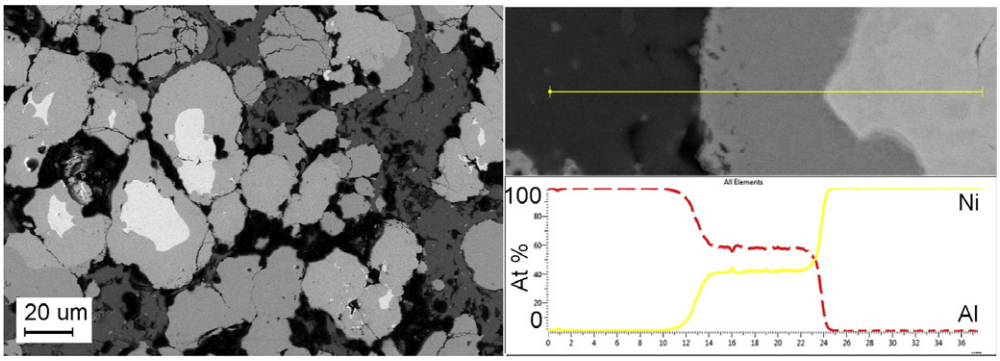

Fig. 9. Microstructure and detail of Ni–Al interphase with linear EDX analysis showing evolution of transient Ni_2Al_3 intermetallic phase after 2 h annealing at 450 °C.

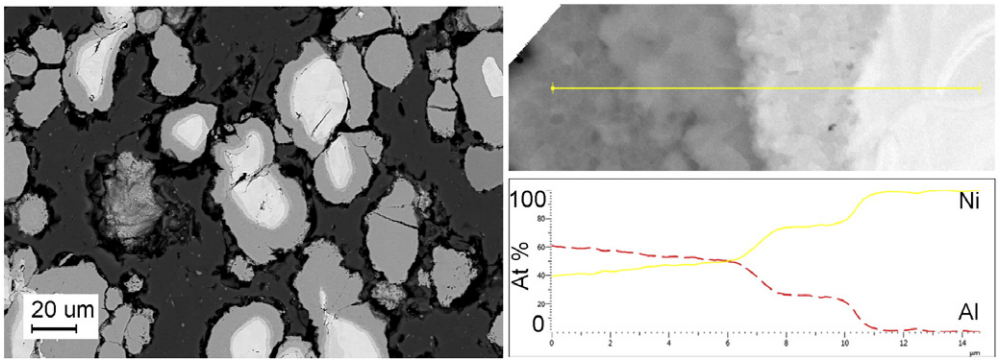

Fig. 10. Microstructure and detail of Ni–Ni_2Al_3 interphase with linear EDX analysis showing gradual evolution of transient Ni_3Al intermetallic phase after 2 h annealing at 500 °C.

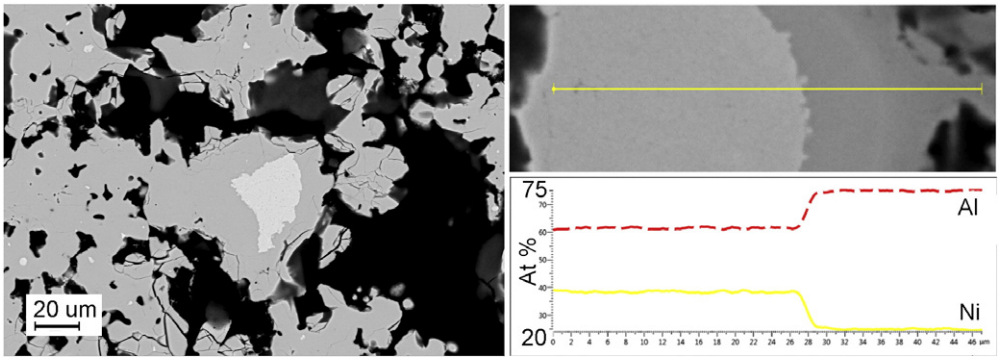

Fig. 11. Microstructure and detail of Ni_2Al_3–$NiAl_3$ interphase with linear EDX analysis after 2 h annealing at 600 °C.

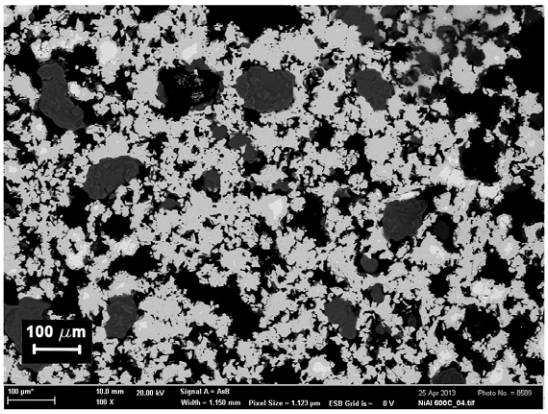

Fig. 12. Microstructure of the intensely reacted Ni–Al deposit after 600 °C/2 h.

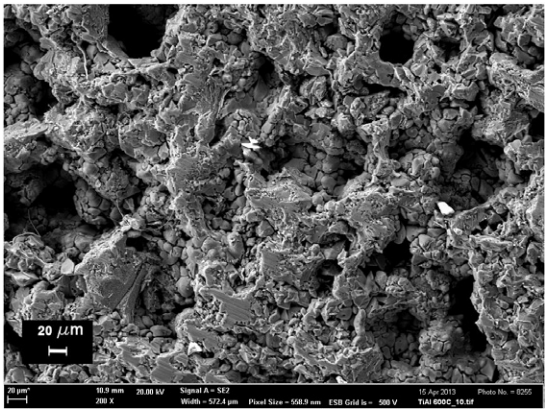

Fig. 13. The open porosity character of the Ni–Al deposit after 600 °C/2 h.

(like Ni_2Al_3) this is probably due to the non-equilibrium nature of the solid phase diffusion reactions.

As these reactions predominantly happen in a solid state, the formation of the new phases is controlled by a mutual diffusion of the two reactants. The high deformation of the deposited material has been be considered as one of the reasons for enhanced diffusivity and therefore for enabling relatively fast creation of intermetallic phases at relatively low temperatures [12]. This results in the formation of porosity generally replacing the former aluminium grains in material [13,14]. As aluminium diffuses in the second constituent (Ni, Ti or Fe), an intermetallic phase is formed and Kirkendall type porosity (in the solid state) arises [15–17]. At a higher temperature of 600 °C, locally some liquid–solid reaction of aluminium rich melt and the still solid second constituent particles could be identified best in the Ni–Al system. The existence of melt even in very small amounts is probably responsible for the fact that after annealing at 600 °C the material is formed purely by intermetallic phases. The analysis of annealed materials showed, that not all of the pure metallic particles have reacted in the FeAl and TiAl samples during 2 h of annealing periods even at 600 °C. This is connected to the solid phase diffusion nature of the reactions.

When aiming for a bulk material, which is usually the ultimate goal of similar studies, porosity is regarded as a negative property (Table 3). In the case of the analysed deposits prepared by cold spray, where no reactions happened during deposition and thus purely bimetallic materials are obtained, the reactions and porosity evolution are allowed in unconstrained nature in all directions. The following porous nature of the annealed materials has the character of open metallic sponge or frame formed by intermetallic phases. The porosity measured by image analysis and density for each of the experimental materials were evaluated and show gradual increase in porosity and decrease in density (Figs. 19, 20, 21).

5. Conclusions

Using CGDS instead of other powder metallurgy methods provides the opportunity to form parts with (nearly) unlimited variability of shapes, which after the proper heat treatment would require only finishing machining operations. Using bi-metallic mixtures, porous intermetallic materials with remnants of original elemental particles were fabricated. Since the open porosity is uniform in size and can be reproduced, the annealed CGDS deposit may be considered to have an interesting new material quality instead of intrinsic microstructure insufficiency. Possible applications of these materials may include infiltration by resin or metallic melt for intermetallic reinforced composite. Also the biocompatibility and the prospective use of these sponges as bone tissue reinforcement parts may be considered.

This intermetallic scaffold can be infiltrated by molten metal to form a metallic–intermetallic composite. Also its use in biomedical applications as reconstructive bone scaffolding can be considered [18]. Since the porosity is open and interconnected, the materials can be used also for gas filtering applications or as a catalyst support.

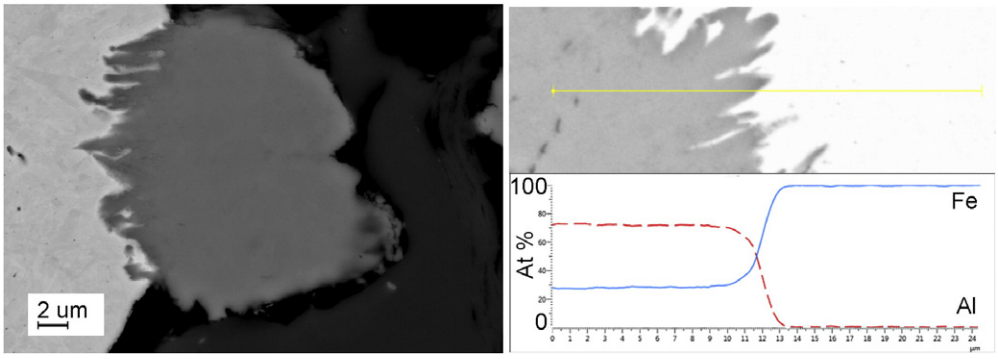

Fig. 14. Microstructure and detail of $FeAl_3$–Fe interphase with linear EDX analysis showing evolution of transient intermetallic phase after 2 h annealing at 500 °C.

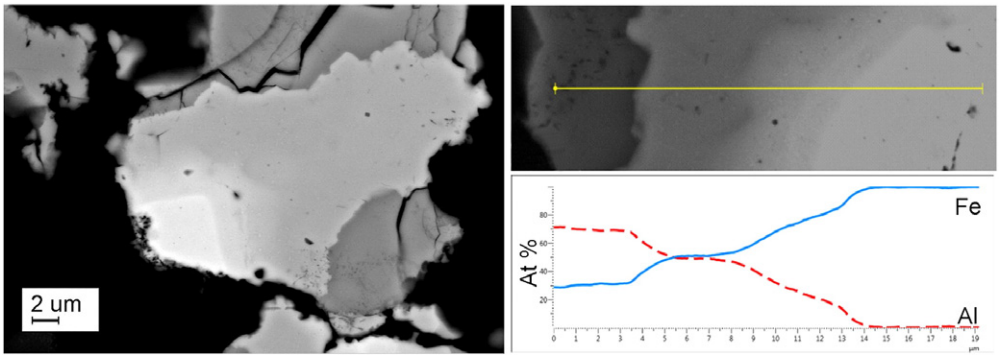

Fig. 15. Microstructure and detail of $FeAl_3$–Fe interphase with linear EDX analysis showing evolution of transient intermetallic phases with FeAl region after 2 h annealing at 600 °C.

Acknowledgments

The present work has been supported by European Regional Development Fund in the framework of the research project NETME Centre under the Operational Programme Research and Development for Innovation (CZ. 1.05/2.1.00/01.0002 ED0002/01/01).

The support of Czech Grant Agency under the project GACR 13-35890S is also acknowledged.

The support of applied research project of the FME BUT FSI-S-11-25 nr 1406 is also appreciated.

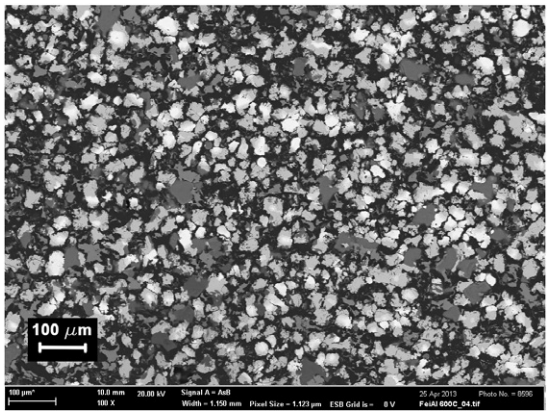

Fig. 16. Microstructure of the FeAl material annealed at 600 °C.

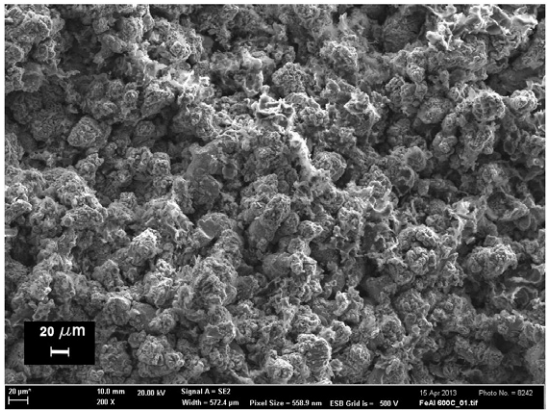

Fig. 17. Porosity on fracture surface of the FeAl material annealed at 600 °C.

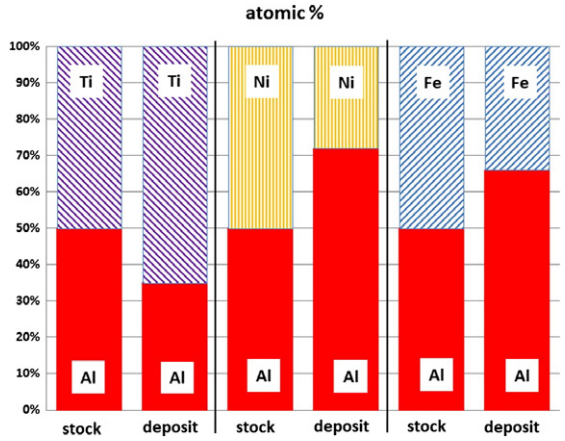

Fig. 18. Change of chemical composition after deposition from 50/50 ratio stock mixtures.

Table 2
Overview of the phases formed at individual temperatures.

°C	Fe–Al deposit	Ni–Al deposit	Ti–Al deposit
300	–	–	(Traces $TiAl_3$), TiAl
450	–	$Ni_3Al + Ni_2Al_3$	$TiAl + TiAl_2$
500	Fe_2Al_5	$Ni_2Al_3 + NiAl + NiAl_3$	$TiAl_3$
550	$FeAl + FeAl_2$	$NiAl_3$	$TiAl + TiAl_2 + TiAl_3$
600	$FeAl + Fe_2Al_5 + Fe_2Al_5$	$NiAl_3$	$TiAl_3 + (TiAl_2 + TiAl + Ti_3Al)$

Table 3
Porosity of samples measured by image analysis on polished cross-sections.

Porosity [%]	As-dep.	300 °C	450 °C	500 °C	550 °C	600 °C
Fe–Al	0.3	3.2	4.8	12.7	16.7	26.7
Ni–Al	0.3	1.2	15.1	23.0	26.2	28.4
Ti–Al	0.4	0.8	2.7	57.5	47.6	55.3

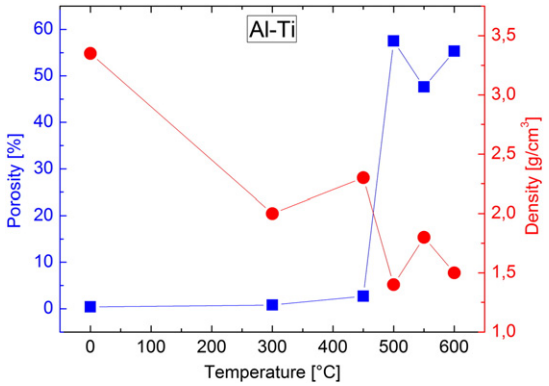

Fig. 19. Porosity and density values for the TiAl deposit as function of the annealing temperatures.

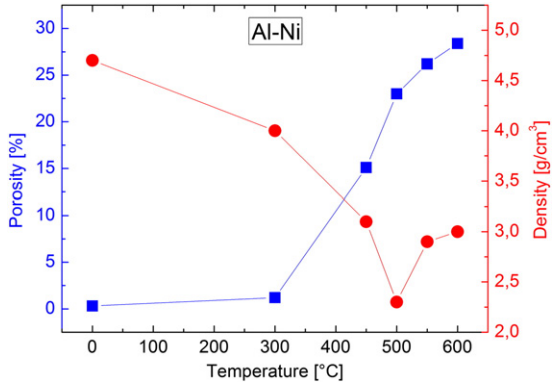

Fig. 20. Porosity and density values for the NiAl deposit as function of the annealing temperatures.

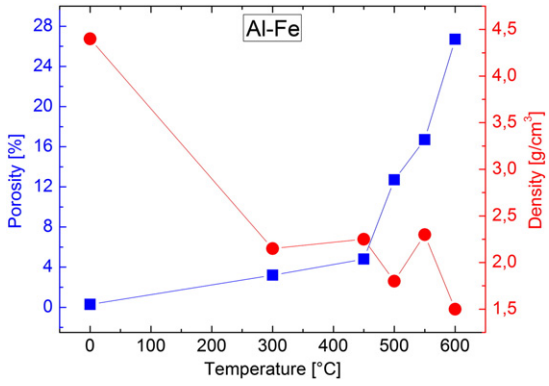

Fig. 21. Porosity and density values for the FeAl deposit as function of the annealing temperatures.

References

[1] F. Gärtner, T. Stoltenhoff, T. Schmidt, H. Kreye, J. Therm. Spray Technol. 15 (2) (2006) 223–232.
[2] S. Marx, A. Paul, A. Köhler, G. Hüttl, J. Therm. Spray Technol. 15 (2) (2006) 177–183.
[3] J.C. Lee, H.J. Kang, W.S. Chu, S.H. Ahn, CIRP Ann. Manuf. Technol. 56 (1) (2007) 577–580.
[4] A.L. Edward, Intermetallics 8 (9–11) (2000) 1339–1345.
[5] G. Dey, Sadhana 28 (1) (2003) 247–262.
[6] E.A. Loria, Intermetallics 9 (12) (2001) 997–1001.
[7] T. Novoselova, P. Fox, R. Morgan, W. O'Neill, Surf. Coat. Technol. 200 (8) (2006) 2775–2783.
[8] T. Novoselova, S. Celotto, R. Morgan, P. Fox, W. O'Neill, J. Alloys Compd. 436 (1–2) (2007) 69–77.
[9] J. Cizek, O. Kovarik, J. Seigl, K.A. Khor, I. Dlouhy, Surf. Coat. Technol. 217 (2013) 23–33.
[10] H. Lee, H. Shin, K. Ko, J. Therm. Spray Technol. 19 (1–2) (2010) 102–109.
[11] H.Y. Lee, S.H. Jung, S.Y. Lee, K.H. Ko, Mater. Sci. Eng. A 433 (1–2) (2006) 139–143.
[12] H.Y. Lee, S.H. Jung, S.Y. Lee, K.H. Ko, Appl. Surf. Sci. 253 (7) (2007) 3496–3502.
[13] M. Mirjalili, M. Soltanieh, K. Matsuura, M. Ohno, Defect Diffus. Forum 322 (2012) 185–194.
[14] U. Kattner, J. Lin, Y. Chang, Metall. Mater. Trans. A 23 (8) (1992) 2081–2090.
[15] L. Xu, Y.Y. Cui, Y.L. Hao, R. Yang, Mater. Sci. Eng. A 435–436 (2006) 638–647.
[16] D.J. Harach, K.S. Vecchio, Metall. Mater. Trans. A 32 (6) (2001) 1493–1505.
[17] Y. Sun, Y. Zhao, D. Zhang, et al., Trans. Nonferrous Metals Soc. China 21 (8) (2011) 1722–1727.
[18] M. Escudero, M. Muñoz-Morris, M. Garćia-Alonso, E. Fernández-Escalante, Intermetallics 12 (3) (2004) 253–260.